NUMERICAL STUDY OF THE RELEASE AND DISPERSION OF A LIGHT GAS USING 3-D CFD CODE GASFLOW-MPI

Han Zhang[1], Jianjun Xiao[2], Yabing Li [3]
[1] Institute of Nuclear and Energy Technologies, Karlsruhe Institute of Technology, 76021 Karlsruhe, Germany, han.zhang@kit.edu
[2] Institute of Nuclear and Energy Technologies, Karlsruhe Institute of Technology, 76021 Karlsruhe, Germany, jianjun.xiao@kit.edu
[3] Institute of Nuclear and Energy Technologies, Karlsruhe Institute of Technology, 76021 Karlsruhe, Germany, uoyerawoh@gmail.com

ABSTRACT

With the development of the hydrogen economy, it requires a better understanding of the potential for fires and explosions associated with the unintended release of hydrogen within a partially confined space. In order to mitigate the hydrogen fire and explosion risks effectively, accurate predictions of the hydrogen transport and mixing processes are crucial. It is well known that turbulence modelling is one of the key elements for a successful simulation of gas mixing and transport. GASFLOW-MPI is a scalable CFD software solution used to predict fluid dynamics, conjugate heat and mass transfer, chemical kinetics, aerosol transportation and other related phenomena. In order to capture more turbulence information, the Large Eddy Simulation (LES) model and LES/RANS hybrid model Detached Eddy Simulation (DES) have been implemented and validated in 3-D CFD code GASFLOW-MPI. The standard Smagorisky SGS model is utilized in LES turbulence model. And the k-epsilon based DES model is employed. This paper assesses the capability of algebraic, k-epsilon, DES and LES turbulence model to simulate the mixing and transport behavior of highly buoyant gases in a partially confined geometry. Simulation results agree well with the overall trend measured in experiments conducted in a reduced scale enclosure with idealized leaks, which shows that all these four turbulent models are validated and suitable for the simulation of light gas behavior. Furthermore, the numerical results also indicate that the LES and DES model could be used to analysis the turbulence behavior in the hydrogen safety problems.

1.0 INTRODUCTION

With a growing interest in the hydrogen-powered systems in the last decade, a number of efforts are made to demonstrate that hydrogen can be used as an energy carrier, such as the mobile and stationary applications. A significant support was given by the international organisations, such as the network HySAFE [1] and IEA [2] and many important progresses were made. Today, the hydrogen safety is still a key issue for practical application. In order to evaluate and mitigate the potential for fires and explosions associated with the unintended release of hydrogen, accurate predictions of the hydrogen transport and mixing processes are crucial. Standard Benchmark Exercise Problems (SBEPs) [3-7] have been proposed to validate the CFD codes for hydrogen-fuelled systems. GASFLOW-MPI is a well-developed parallel scalable CFD software solution to predict the fluid dynamics, conjugate heat and mass transfer, chemical kinetics, aerosol transportation and other related physical processes, which are the key physical phenomena in the hydrogen safety analysis [8]. Furthermore, GASFLOW has been validated by blind-/open-international benchmarks and widely used to analyse the hydrogen distribution and risk mitigation [9-16]. It is well known that turbulence modelling is one of the key elements for a successful simulation of hydrogen transport and mixing processes. In this paper, the hydrogen jets simulation in a partially confined space, which is one of the typical scenarios encountered in risk analyses for the future hydrogen energy carrier, is performed by the parallel scalable CFD software GASFLOW-MPI. Several turbulent models, including algebraic model, k-epsilon model, DES model and LES model, are employed and their computational performances are compared.

This paper is organized as follows. The conservation equations in GASFLOW-MPI are introduced in section 2, and then, the outline of the turbulent models are described in section 3. The numerical results are presented and discussed in section 4. The conclusions are presented in section 5.

2.0 CONSERVATION EQUATION

Volume equation

$$\frac{\partial V}{\partial t} = V\nabla\cdot(\mathbf{b}-\mathbf{u}) \tag{1}$$

where $\mathbf{u}$ is the fluid velocity vector, V is the discretized fluid control volume and $\mathbf{b}$ is the control volume velocity surface vector incorporated in the simplified ALE methodology used in GASFLOW-MPI. When $\mathbf{b}$=0 the equations are in Eulerian coordinates, and when $\mathbf{b}$=$\mathbf{u}$ the equations are in Lagrangian coordinates.

Mass equation

$$\frac{\partial \rho}{\partial t} = \nabla\cdot\left[\rho(\mathbf{b}-\mathbf{u})\right] \tag{2}$$

where ρ is the mixed fluid density.

Individual species mass equation

$$\frac{\partial \rho_a}{\partial t} = \nabla\cdot\left[\rho_a(\mathbf{b}-\mathbf{u})\right] + \nabla\cdot\mathbf{J}_a + \nabla\cdot\tilde{\mathbf{J}}_a \tag{3}$$

where ρ_a is the density of species a, $\mathbf{J}_a$ is the mass diffusion flux vector of species a, and $\tilde{\mathbf{J}}_a$ is the turbulent mass diffusion flux vector which should be modelled by the turbulent model. The turbulent turbulent mass diffusion flux vector is modelled using the gradient hypothesis, as Eq.(4), and calculated by employing a turbulent Schmidt number Sc_t, as Eq. (5).

$$\mathbf{J}_a + \tilde{\mathbf{J}}_a = \rho_a\left(D_a + \tilde{D}_a\right)\nabla\left(\rho_a/\rho\right) \tag{4}$$

$$\tilde{\mathrm{D}}_a = \frac{\mu_t}{\rho_a Sc_t} \tag{5}$$

Momentum equation

$$\frac{\partial(\rho\mathbf{u})}{\partial t} = \nabla\cdot\left[\rho\mathbf{u}(\mathbf{b}-\mathbf{u})\right] - \nabla p + \rho\mathbf{g} + \nabla\cdot\boldsymbol{\sigma} + \nabla\cdot\tilde{\boldsymbol{\sigma}} \tag{6}$$

where p is the pressure, $\boldsymbol{\sigma}$ is the viscous stress tensor, $\mathbf{g}$ is the gravitational vector, and $\tilde{\boldsymbol{\sigma}}$ is the Reynolds stresses term which should be modelled by the turbulent model. The Boussinesq hypothesis is employed to model the turbulent stresses, as shown in Eq.(7) and (8). $\mathbf{S}$ is the the rate-of-strain tensor. Different turbulent models are employed to calculate the turbulent viscosity coefficient μ_t.

$$\boldsymbol{\sigma}_{ij} + \tilde{\boldsymbol{\sigma}}_{ij} = -2(\mu+\mu_t)\left(S_{ij} - \frac{1}{3}S_{kk}\delta_{ij}\right) \tag{7}$$

$$S_{ij} = \frac{1}{2}\left(\frac{\partial u_i}{\partial x_j} + \frac{\partial u_j}{\partial x_i}\right) \tag{8}$$

Internal energy equation

$$\frac{\partial(\rho I)}{\partial t} = \nabla\cdot\left[\rho I(\mathbf{b}-\mathbf{u})\right] - p\nabla\cdot\mathbf{u} - \mathbf{q} - \tilde{\mathbf{q}} \tag{9}$$

where I is the fluid internal energy, $\mathbf{q}$ is the energy flux vector and $\tilde{\mathbf{q}}$ is the turbulent heat flux term. The term $\tilde{\mathbf{q}}$ is the second term which should be modelled by the turbulent model. The turbulent heat flux term is modelled using the similar method in the turbulent turbulent mass diffusion flux vector, as Eq.(10), and calculated by employing a turbulent Prandtl number Pr_t, as Eq. (11).

$$\mathbf{q}+\tilde{\mathbf{q}}=\left(\lambda+\lambda_t\right)\nabla T \tag{10}$$

$$\lambda_t=\frac{\rho\mu_t}{\mathrm{Pr}_t} \tag{11}$$

3.0 TURBULENT MODEL

Four turbulent models are employed in this paper. Algebra model and k-epsilon model are RANS-based turbulent model which are well-accepted in industry applications. Recently, the Large Eddy Simulation (LES) model and Detached Eddy Simulation (DES) model are developed and validated to capture more details of turbulence and flow features in applications of scientific research and engineering problems.

3.1 Algebraic Model

Algebraic turbulence model is also called as zero-equation turbulence model, which does not require the solution of any additional turbulence transport equations. The turbulent viscosity coefficient μ_t is calculated directly from the current flow variables, as shown in Eq.(12). As a result, history effects of turbulence may not be able to properly account in Algebraic turbulence model, such as convection and diffusion of turbulent energy.

$$\mu_t=C_\mu\rho k^{1/2}l \tag{12}$$

Where $C_\mu=0.05$

3.2 K-epsilon Model

K-epsilon turbulence model [18] is one of the most common model to simulate the mean characteristics of the turbulent flow. It is a kind of two equation models which gives a general description of turbulence by turbulence energy transport equation and turbulence dissipation rate equation, as shown in Eq.(13) and (14). The turbulent viscosity coefficient μ_t is calculated by Eq.(15).

$$\frac{\partial}{\partial t}\left(\rho k\right)+\nabla\cdot\left(\rho k\mathbf{U}\right)=\nabla\cdot\left[\left(\mu+\frac{\mu_t}{\sigma_k}\right)\nabla k\right]+G_k+G_b-\rho\varepsilon \tag{13}$$

$$\frac{\partial}{\partial t}\left(\rho\varepsilon\right)+\nabla\cdot\left(\rho\varepsilon\mathbf{U}\right)=\nabla\cdot\left[\left(\mu+\frac{\mu_t}{\sigma_\varepsilon}\right)\nabla\varepsilon\right]+C_{\varepsilon1}\frac{\varepsilon}{k}\left(G_k+G_b\right)-C_{\varepsilon2}\rho\frac{\varepsilon^2}{k} \tag{14}$$

$$\mu_t=\rho C_\mu\frac{k^2}{\varepsilon} \tag{15}$$

C_1	C_2	C_μ	σ_k	σ_ε
1.44	1.92	0.09	1.0	1.3

3.3 Detached Eddy Simulation Model

Detached Eddy Simulation (DES) model is a kind of RANS/LES hybrid turbulence model [19]. The main feature of DES model is that it could switch between RANS and LES adaptively according to the local turbulent information. When the mesh size is fine enough to resolve the turbulent information, the DES model approaches to the LES model. In the opposite condition, DES model approaches to the k-epsilon model. In this paper, the k-epsilon based DES model is employed to model the turbulence behavior, as shown in Eq.(16) ~ (19).

$$\frac{\partial}{\partial t}\left(\rho k\right)+\nabla\cdot\left(\rho k\mathbf{U}\right)=\nabla\cdot\left[\left(\mu+\frac{\mu_t}{\sigma_k}\right)\nabla k\right]+G_k+G_b-\frac{\rho k^{3/2}}{l_{des}} \tag{16}$$

$$\frac{\partial}{\partial t}\left(\rho\varepsilon\right)+\nabla\cdot\left(\rho\varepsilon\mathbf{U}\right)=\nabla\cdot\left[\left(\mu+\frac{\mu_t}{\sigma_\varepsilon}\right)\nabla\varepsilon\right]+C_{\varepsilon 1}\frac{\varepsilon}{k}\left(G_k+G_b\right)-C_{\varepsilon 2}\rho\frac{\varepsilon^2}{k} \tag{17}$$

$$l_{des}=\min\left(l_{rke},l_{les}\right),\quad l_{rke}=\frac{k^{3/2}}{\varepsilon},\quad l_{les}=\mathrm{C}_{des}\Delta_{\max},\quad \Delta_{\max}=\max\left(\Delta x,\Delta y,\Delta z\right) \tag{18}$$

$$\mu_t=\rho C_\mu\frac{k^2}{\varepsilon} \tag{19}$$

Where $\mathrm{C}_{des}=0.65$

3.4 Large Eddy Simulation Model

Different form the RANS model, most of the turbulent fluctuation could be resolved directly in LES and only the turbulence eddy at sub-grid scale should be modeled by sub-grid scale model. The Smagorinsky model is employed in GASFLOW-MPI to calculate the SGS turbulent viscosity due to its simplicity and practicality [20]. And the turbulent viscosity could be expressed by Eq. (20).

$$\mu_t=\rho L_s^2\left|S\right| \tag{20}$$

$$L_s=C_s\Delta \tag{21}$$

$$\Delta=V^{1/3}=\left(\Delta x\Delta y\Delta z\right)^{1/3} \tag{22}$$

$$\left|S\right|=\sqrt{2S_{ij}S_{ij}} \tag{23}$$

Where $\mathrm{C}_s=0.1$

4.0 NUMERICAL RESULTS

4.1 Problem Description

A series of experiments [17] were performed to characterize the mixing and dispersion of light gas in a partially confined space and to develop a database using for CFD validation. In this paper, a reduced scale two-car residential garage with interior dimensions of 1.5 m × 1.5 m × 0.745 m was employed, as shown in Fig.1. Due to safety concerns, helium was used instead of hydrogen in this experiment.

The helium was released into the compartment from the burner with specified velocity of 14.95 L/min for one hour and then 3.74 L/min for the next hour. It should be noted that the term burner used here only means a device that releases helium, but no chemical reaction occurs. In this experiment, the height of the burner was 207 mm and the exit diameter was 36 mm. And seven sensors were employed to measure the time-resolved helium volume fractions at different heights, which located at one horizontal location (35.5 cm from front and 40.5 cm from side) within the compartment, as shown in Fig.1. The vertical location of each sensor was also indicated in Fig.1. In a typical garage, there were always several small leaks especially near the garage door and windows which was represented by a hole on the wall in this experiment, as shown in Fig.1.

According to the experiment configuration, the computational domain is set as following. There is 1.5 m in the x direction and y direction, respectively, and 0.75 m in z direction. The uniform grid spacing is selected for z directions and a non-uniform mesh is employed for the x direction and y direction which are refined to resolve the turbulent information near the burner. The minimum mesh size in x and y direction is about 0.78 cm. And the mesh size reach the maximum value at the outer surface. The number of grid points is equal to 74 × 64 × 32 points in the x, y, and z direction, respectively.

For the inlet boundary at the burner, the fixed velocity boundary condition is utilized according to the specified velocity in the experiment. Zero-gradient boundary, also called continuous boundary condition, is posed at the hole near on the wall. The no-slip boundary condition is employed on the other walls, as shown in Fig. 1.

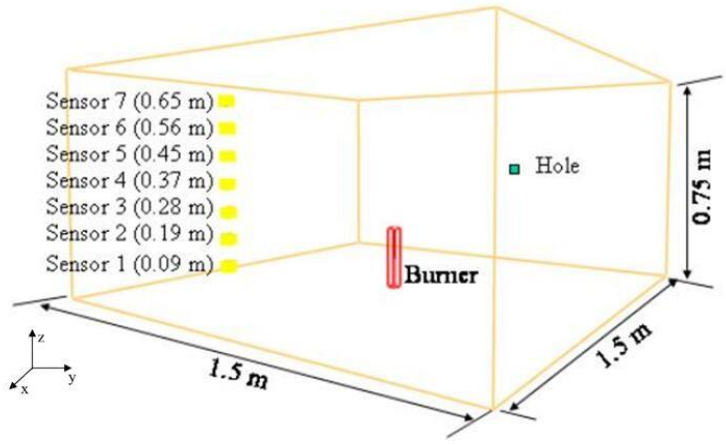

Fig.1 Experiment configuration [17]

4.2 Results and Discussion

Fig. 2 shows helium volume fraction distribution on a y-z plane passing through the middle of the burner at 2000 s where the k-epsilon turbulent model is employed. After released from the burner, the buoyant helium plume rose up to the ceiling and then propagated horizontally. The high helium concentration is built up close to the ceiling. The original air near the ceiling was compressed into the lower part and partial air was pushed out through the hole in the wall. Helium at the high concentration region also diffused to downward due to the helium concentration gradient. With the help of diffusion effect, there is a small helium volume fraction variation in the horizontal direction at the region far away from the plume. After the release phase (0~3600 s), the results indicated that the helium volume fraction distribution in the entire compartment became quite uniform due to the concentration diffusion, based on the data for 5400 s, as shown in Fig. 3. Only a small helium volume fraction gradient exists in the vertical direction under the action of gravity.

In this section, experimental data of helium concentration at seven sensor locations is discussed firstly. And then the comparison between experimental data (symbols) and numerical predictions (lines) using four turbulent models is presented, as shown in Fig.4-Fig.7. For the experiment data [17], the sensor 7 (black) located closest to the ceiling reaches a peak volume fraction of approximately 0.47 at the 3600 s, when the helium flow is stopped releasing through the burner. A similar phenomenon is observed at the sensor 4-6 whose concentration profile shows a peak at 3600 s. While, the volume fraction at sensors 1-3 continues to rise even after the end of the release phase. It is because that the helium at the high concentration region diffuses towards the floor during the period between 3600 s and 7200 s.

Under the effect of the diffusion, the helium concentration measured by different sensor becomes quite uniform whose value is about 0.39 at 7200 s.

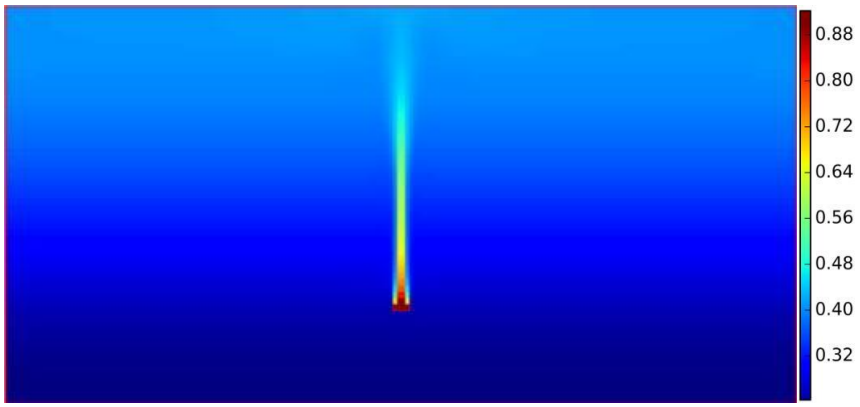

Fig.2 Helium volume fraction at 2000 s (y-z plane)

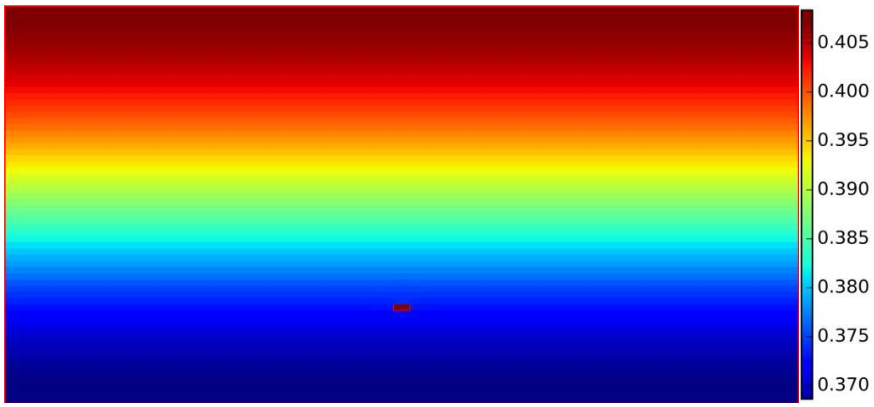

Fig.3 Helium volume fraction at 5400 s (y-z plane)

Simulation results of four turbulent model agree well with the overall trend measured in experiments. The numerical results show that concentration profiles at sensor 4-7 reach a peak at 3600 s. The concentration profiles at sensor 1-3 continue to rise during the whole process. At 7200 s, the helium concentrations at different sensor becomes quite uniform whose value is consistent with the experimental value. However, there are two relative large differences between the experimental data and simulation results. One occurs in the sensor 7 during the period between 1600 s and 2000 s. The other one occurs at the sensor 1 during the period between 3600 s and 4000 s when the helium flow through the burner is stopped. The possible reason is that the uncertainty in the experimental measurement.

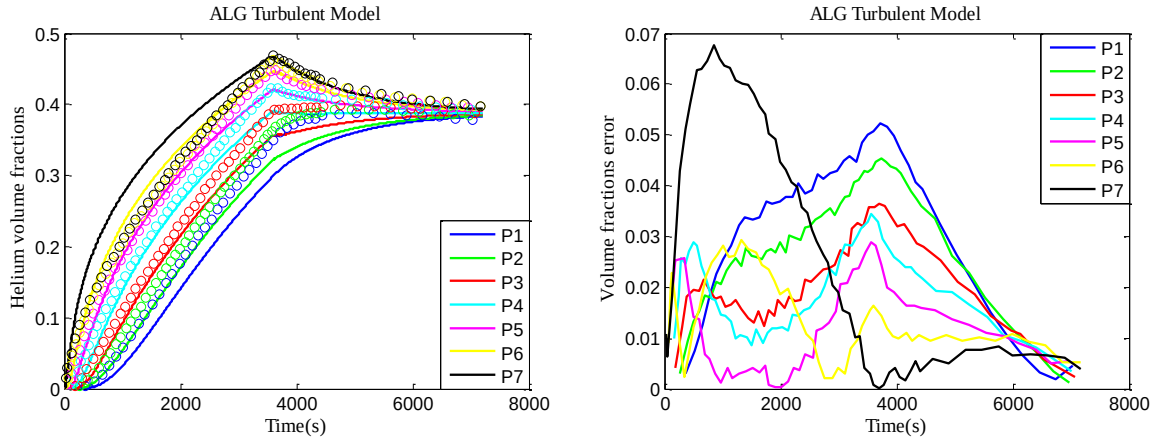

Fig.4 Algebraic turbulent model simulation results

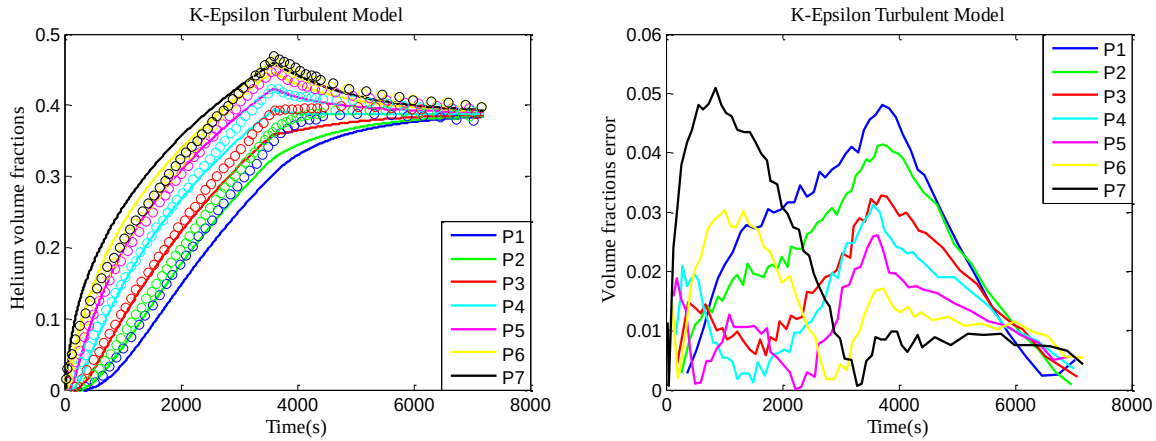

Fig.5 K-epsilon turbulent model simulation results

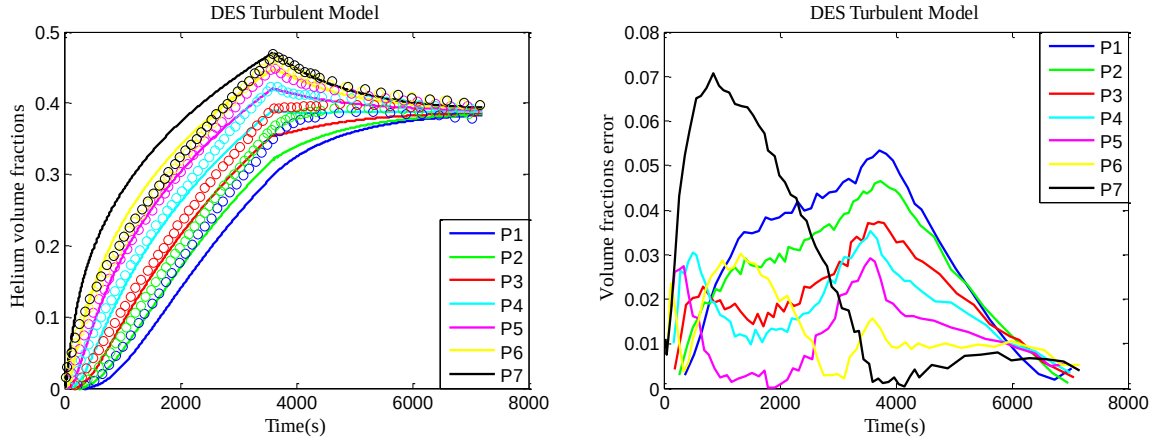

Fig.6 DES turbulent model simulation results

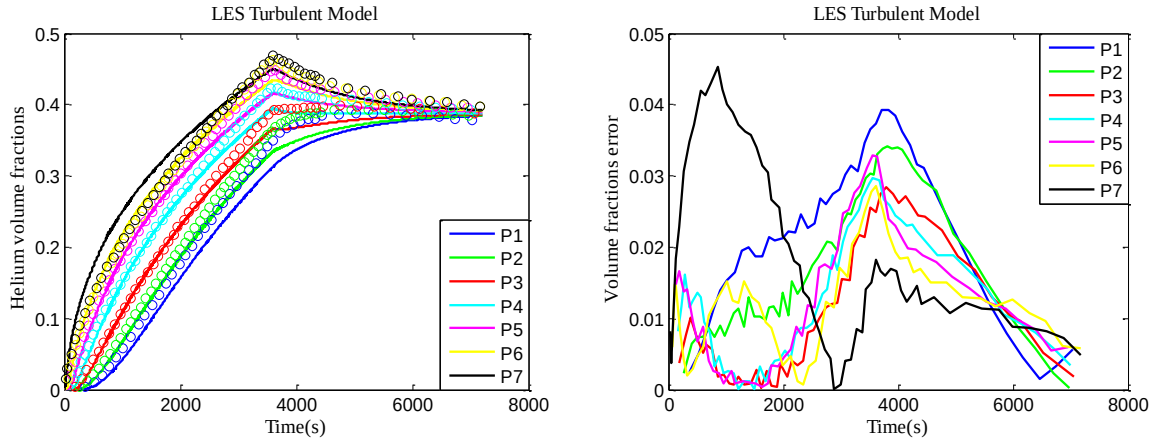

Fig.7 LES turbulent model simulation results

5.0 CONCLUSION

In this paper, the Large Eddy Simulation (LES) model and Detached Eddy Simulation (DES) have been developed in 3-D CFD code GASFLOW-MPI to capture more turbulence information. In particular, the standard Smagorisky SGS model is utilized to resolve the turbulence behavior at subgrid scale in LES turbulence model. And the k-epsilon based DES model is employed to switch between RANS and LES adaptively. The validation of algebraic, k-epsilon, DES and LES turbulence model is performed in this paper by simulating the mixing and transport behavior of highly buoyant gases. Simulation results agree well with the overall trend measured in experiments conducted in a reduced scale enclosure. Furthermore, the numerical results also indicate that the newly developed LES and DES model could be used to analysis the turbulence behaviour in the hydrogen safety problems. In the future, the new developed turbulent models will be further validated and applied for the hydrogen safety analysis.

REFERENCES

1. https://www.iea.org/
2. http://www.hysafe.org/
3. HySafe Deliverable D75, List of Basic Test Problems, WP6, FZK.
4. HySafe Deliverable D81, Specifications of the set of SBEPs for the 4th period, WP6, FZK.
5. HySafe Deliverable D88, Compilation report on SBEPs results of the 4th period, WP6, FZK.
6. HySafe Deliverable D107, Specifications of the set of SBEPs for the 5th period, WP6, FZK.
7. HySafe Deliverable D115, SBEP data base, WP6, FZK.
8. Xiao, J., Travis, J., Royl, P., Necker, G., Svishchev, A., and Jordan, T., GASFLOW-MPI: A Scalable Computational Fluid Dynamics Code for Gases, Aerosols and Combustion. Theory and Computational Model, vol. 1. KIT Report. 2011.
9. Royl, P., Müller, C., Travis, J.R., Wilson, T., Validation of GASFLOW for Analysis of Steam/Hydrogen Transport and Combustion Processes in Nuclear Reactor Containments, Procs 13th Conference on Structural Mechanics in Reactor Technology, Porto Alegre, RS, Brazil, 1995.
10. Royl, P., Travis, J.R., Breitung, W., Benchmarking of the 3D CFD Code GASFLOW with Containment Thermal Hydraulic Tests from HDR and ThAI, procs IAEA-OECD CFD4NRS Conference, 2006.
11. Royl, P., Necker, G., Spore, J.W., Travis, J.R., 3D Analysis of Hydrogen Recombination Experiments in the Battelle Model Containment with the GASFLOW Code, Procs Jahrestagung Kerntechnik, Munich, 1998.

12. Allelein, H.J., et al, International Standard Problem ISP-47 on Containment Thermal Hydraulics, OECD -final report, 2006.
13. Xiao, J., Travis, J.R., How critical is turbulence modeling in gas distribution simulations of largescale complex nuclear reactor containment? , Annals of Nuclear Energy, Vol 56, 227-242, 2013.
14. Xiao, J., Breitung, W., Kuznetsov, M., GASFLOW-MPI: A new 3-D parallel all-speed CFD code for turbulent dispersion and combustion simulations: Part I: Models, verification and validation, International Journal of Hydrogen Energy, Available online 18 March 2017.
15. Xiao, J., Breitung, W., Kuznetsov, M., GASFLOW-MPI: A new 3-D parallel all-speed CFD code for turbulent dispersion and combustion simulations Part II: First analysis of the hydrogen explosion in Fukushima Daiichi Unit 1, International Journal of Hydrogen Energy, Available online 18 March 2017.
16. Zhang, H., Xiao, J., Direct Numerical Simulation and Large Eddy Simulation of a Flow at Low Reynolds Number over Backward-Facing Step Using CFD Code GASFLOW-MPI, NUTHOS-11, Gyeongju, Korea, October 9-13, 2016.
17. William Pitts, Kuldeep Prasad Jiann Yang, Experimental Characterization and Modeling of Helium Dispersion in a 1/4 –Scale Two-Car Residential Garage, 3rd International Conference on Hydrogen Safety, 2009.
18. B. E. Launder and D. B. Spalding, Lectures in Mathematical Models of Turbulence. Academic Press, London, England. 1972.
19. P.R. Spalart, Detached-eddy simulation. Ann. Rev. Fluid Mech. 41, 181–202, 2009.
20. J. Smagorinsky, General Circulation Experiments with the Primitive Equations. I. The Basic Experiment. Month. Wea. Rev.. 91. 99–164. 1963.